



# QUANTUM-DOT DEVICES AND QUANTUM-DOT CELLULAR AUTOMATA

WOLFGANG POROD

*Department of Electrical Engineering,  
University of Notre Dame,  
Notre Dame, IN 46556, USA*

Received June 26, 1996; Revised February 16, 1997

We discuss novel nanoelectronic architecture paradigms based on cells composed of coupled quantum-dots. Boolean logic functions may be implemented in specific arrays of cells representing binary information, the so-called *Quantum-Dot Cellular Automata* (QCA). Cells may also be viewed as carrying analog information and we outline a network-theoretic description of such *Quantum-Dot Nonlinear Networks* (Q-CNN). In addition, we discuss possible realizations of these structures in a variety of semiconductor systems (including GaAs/AlGaAs, Si/SiGe, and Si/SiO<sub>2</sub>), rings of metallic tunnel junctions, and candidates for molecular implementations.

## 1. Introduction

Since its inception a few decades ago, silicon ULSI technology has experienced an exponential improvement in virtually any figure of merit. However, there are indications now that this progress will slow, or even come to a standstill, as technological and fundamental limits are being reached. This slow-down of conventional silicon technology may provide an opportunity for alternative device technologies. In this paper, we will describe some ideas of the *Notre Dame NanoDevices Group* on a possible future nanoelectronic computing technology based on cells of coupled quantum dots.

Up until today, silicon technology has closely followed a famous dictum made in 1965 by Intel Corporation chairman Gordon Moore. In those early days of the integrated circuit, he had projected the expected progress for the next decade, anticipating that the number of transistors on a chip and their performance would double every 18 months, or so. Now, three decades later, this prediction has turned out to be remarkably accurate over the whole duration. Figure 1 gives a schematic version of this so-called *Moore's Law*, the solid line showing the exponential reduction in the minimum

feature size over the past 30 years. For how long will this trend continue?

In recent years, the Semiconductor Industry Association has studied this question and issued a blueprint for future development which has become known as the *SIA Roadmap* [1994]. Basically, the *Roadmap* predicts a continuation of *Moore's Law* early into the next century. However, there is an increasing indication that these improvements will not continue when we enter the deep submicron or nanometric regime. Both technological and fundamental limitations will be responsible for the anticipated slow-down and eventual standstill. It is expected that by the year 2010, minimum feature sizes will be on the order of 0.07 micrometer, or 70 nanometer ( $10^3 \text{ nm} = 1 \mu\text{m} = 10^{-6} \text{ m}$ ).

Among the chief technological limitations responsible for this expected slow-down are the interconnect problem and power dissipation [Keyes, 1987; Ferry *et al.*, 1987, 1988]. As more and more devices are packed into the same area, the heat generated during a switching cycle can no longer be removed, and the chip literally begins to melt. Interconnections do not scale in concert with device scaling because of the effect of wire resistance and capacitance, giving rise to a wiring bottleneck. It is

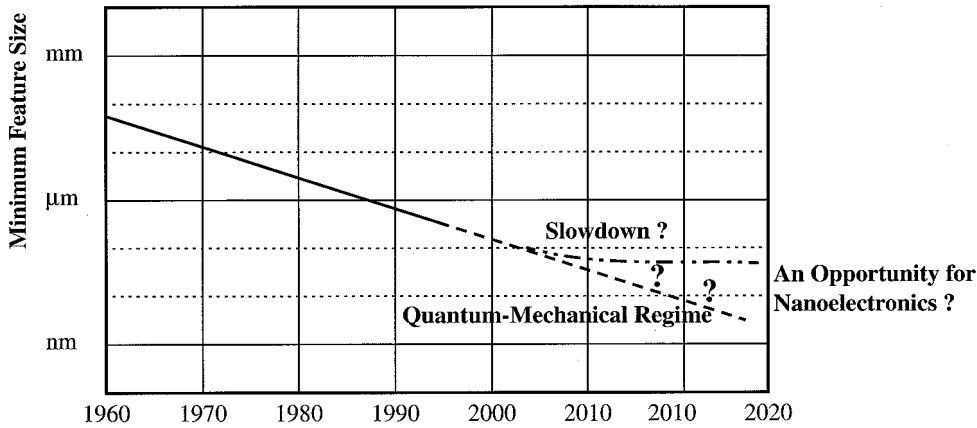


Fig. 1. Schematic version of Moore’s Law showing the exponential reduction in the minimum feature size for the past three decades (solid line) and its extrapolation into the next century (dashed line).

generally recognized that alternate approaches are needed to create innovative technologies that provide greater device and interconnect functionality per lithography feature, thus lessening the dependence on simple scaling, or to utilize innovative circuit and system architectural features that provide more function per transistor.

Fundamental limits arise as device dimensions shrink due to changes in device performance dictated by the laws of physics. These phenomena include a loss of gate control and quantum mechanical effects as devices enter the nanometer regime. Current CMOS technology is based on devices which basically act as voltage-controlled current switches. In the deep submicron regime, the required gate control will no longer be possible because of short-channel effects due to electrostatics. Device operation will also be altered due to the emerging quantum mechanical nature of the electrons, thus giving rise to novel physical effects.

Because of the above reasons, expectations are that potential show-stoppers await conventional silicon ULSI as it approaches the nanometer regime. Scaled-down transistors interconnected in conventional circuit architectures will no longer function as required and the fabrication will pose insurmountable problems. However, these obstacles for silicon circuitry may present an opportunity for alternative device technologies which are designed for the nano-regime and which are interconnected in an appropriate architecture. This is the main “vision” of this paper.

In this paper, we describe our ideas of using nanostructures (more specifically, quantum dots) which are arranged in locally-interconnected

cellular-automata-like arrays. We will demonstrate that suitably constructed structures may be used for computation and signal processing. Our proposal is called “Quantum-Dot Cellular Automata” (QCA) [Lent *et al.*, 1993]. Note that our proposal is not a quantum computer in the sense of the “quantum computing” community, as reviewed by Spiller [1996]. QCA’s do not require quantum mechanical phase coherence over the entire array; phase coherence is only required inside each cell and the cell-cell interactions are classical. This limited requirement of quantum mechanical phase coherence makes QCA’s a more attractive candidate for actual implementations.

Our work is based on the highly advanced state-of-the-art in the field of nanostructures and the emerging technology of quantum-dot fabrication [Weisbuch & Vinter, 1991; Kelly, 1995; Turton, 1995; Montemerlo *et al.*, 1996]. As

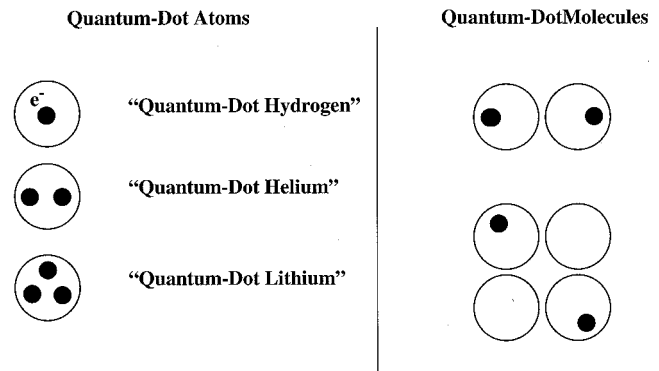


Fig. 2. Schematic diagram of artificial “quantum-dot atoms” and “quantum-dot molecules” which are occupied by few electrons.

schematically shown in Fig. 2, several groups have demonstrated that electrons may be completely confined in semi-conductor nanostructures, which may then be thought of as artificial “semi-conductor atoms”. Controllable occupation of these quantum dots has been achieved in the few-electron regime. One may speak of “quantum-dot hydrogen”, “quantum-dot helium”, “quantum-dot lithium”, etc. [Kastner, 1993; Ashoori, 1996]. Very recently, coupling between quantum-dot atoms in close proximity has been observed, thus realizing artificial “quantum-dot molecules”.

In order to observe quantization phenomena, extremely pure material is needed and the experiments have to be done at very low temperatures using cryogenic techniques [Weisbuch & Vinter, 1991]. The reason for this is that quantum-mechanical coherence is destroyed by scattering due to both impurities (thus the requirement of highly pure material) and lattice vibrations (thus the requirement of low temperature). While low temperatures are not desirable for purposes of applications, they reflect the current technological limitation in the fabrication of nano-meter-size structures [Kelly, 1995]. Any decrease in the feature sizes will result in less stringent requirements for purity and low temperature. Control on the molecular level, i.e. molecular electronics implementations, would make possible room temperature operation.

We are led to consider quantum dots for device applications. This will entail a need for new circuit architecture ideas for these new devices. The nanostructures we envision will contain only few electrons available for conduction. It is hard to imagine how devices based on nanostructures could function in conventional circuits, primarily due to the problems associated with charging the interconnect wiring with the few electrons available. Therefore, we propose to envision a nanoelectronic architecture where the information is contained in the arrangement of charges and not in the flow of charges (i.e. current). In other words, the devices interact by direct Coulomb coupling and not by currents through wires. We envision to utilize the existing physical interactions between neighboring devices in order to directly produce the dynamics, such that the logical operation of each cell would require no additional connections beyond the physical coupling within a certain range of interactions. We are led to consider cellular-automata-like device architectures of cells communicating with each other by their Coulombic interaction.

Figure 3 schematically shows a locally-interconnected array consisting of cells of nano-electronic devices. The physical interactions together with the array topology determine the overall functionality. “What form must a cellular array take when its dynamics should result directly from known physical interactions?”. If we simply arrange nanometer-scale devices in a dense cellular array, the device cells may interact, but we have given up all control over which cell interacts with which neighbor and when they interact. In general, the state of a cell will depend on the state of its neighbors within a certain range. The main questions now are: “What functionality does one obtain for a given physical structure?” and “Given a certain array behavior, is there a physical system to implement it?”.

This problem of a desired mapping between local connection rules and overall array behavior is an old one, and known to be difficult. No general principles exist which would allow one to extrapolate “interesting” array dynamics from a given set of interactions. A two-pronged approach suggests itself to tackle this problem: In the “top down approach” the functionality of the array is first specified, and then one faces the problem of realizing the required local connectivities. On the other hand, in a “bottom up approach” the physical pattern of interconnections is given, and one then attempts to infer possible overall behavior of the array.

Computation in physics-like cellular spaces has been studied over the years. Konrad Zuse, a German computer pioneer, investigated the behavior of discrete-space and discrete-time systems, which he termed “Rechnender Raum” (translated as “Computing Space”) [Zuse, 1969]. He showed that a binary space (two states per cell) with an appropriate dynamical law support the propagation of

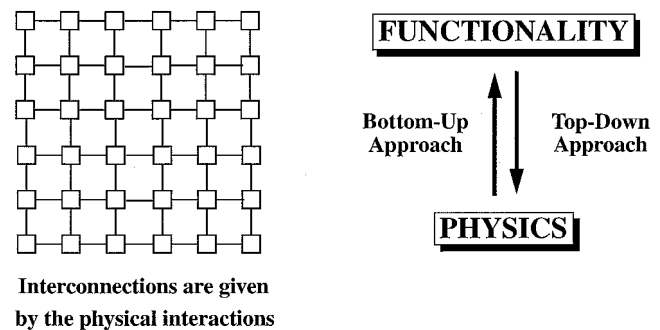


Fig. 3. Schematic picture of a cellular array where the interconnections are given by physical law. The underlying physics determines the overall functionality of the array.

elementary patterns, which he called “Digital-Teilchen” (“Digital Particle”). The idea that “discrete” cellular spaces might provide an alternative to “continuous” classical physics has been discussed by Toffoli and Margolus [1987]. Frisch, Hasslacher, and Pomeau [1986] showed that deterministic lattice gases with discrete Boolean elements are able to simulate the Navier–Stokes equation. Biafore has proposed so-called replica cellular automata for nanometer scale computation [1994]. We have studied this relationship between local connectivity patterns with overall array behavior, using the discretized Helmholtz equation as a computational model [Porod, Harbury & Lent, 1996]. Using continuous cell states, one obtains wave phenomena like Huygen’s principle, diffraction, and interference. For discrete cell states, the resulting switching rules are very similar to the ones used by Konrad Zuse in his pioneering work on discrete spacetime models of computation.

In the following chapters we will develop these ideas in detail and we will present a concrete example of a quantum-dot cell with an appropriate architecture, the so-called Quantum-Dot Cellular Automata. We will discuss how one may construct QCA cells that encode binary information and how one can thus realize Boolean logic functions. We will also discuss how one may view these arrays as quantum-dot cellular neural (or, nonlinear) networks Q-CNN’s. A key question, of course, are implementations. We will discuss ideas (and on-going work) on attempting to implement these structures in a variety of semiconductor systems (including GaAs/AlGaAs, Si/SiGe, and Si/SiO<sub>2</sub>) and also metallic dots. Alternative implementations include molecular structures. We will call attention to a specific molecule which appears to be particularly promising since it possesses a structure similar to a QCA cell. One of the most promising material systems appears to be Si/SiO<sub>2</sub>, mostly due to the excellent insulating properties of the oxide. Note that our search for a technology beyond silicon may bring us back to silicon!

Exciting as the vision of a possible nanoelectronics technology may be, many fundamental and technological challenges remain to be overcome. We should keep in mind that this exploration has just begun and that other promising designs remain yet to be discovered. This exciting journey will require the combined efforts of technologists, device physicists, circuit-and-systems theorists, and computer architects.

## 2. Introduction to Nanoelectronic Structures

Here we attempt to provide a state-of-the-art survey of nanofabrication, i.e. the realization of electronic devices on the nanometer scale. In this regime, quantum mechanical effects become visible and may be exploited for device functionality [Capasso, 1990]. In these small structures, device performance is determined by only a few electrons, and in the limit by only a single electron per device [Grabert & Devoret, 1992]. Our focus in particular will be on a review of quantum-dot fabrication techniques for the design and realization of artificial semiconductor quantum-dot atoms and molecules [Kastner, 1993; Ashoori, 1996].

### 2.1. Low-dimensional semiconductor structures

Advanced semiconductor growth techniques, such as molecular beam epitaxy (MBE), allow the fabrication of semiconductor sandwich structures with interfaces of virtually atomic precision. This control in the growth direction allows one to realize artificial layered crystals with desired electronic and optical properties, as first suggested by Esaki and Tsu [1970]. A schematic picture of such a sandwich structure is shown in Fig. 4. The various layers can be made to possess different properties by choosing an appropriate material during growth. One of the main uses of this technique is to utilize the difference in bandgap between materials in the various layers. This difference in the band gap results in an effective electronic potential energy which

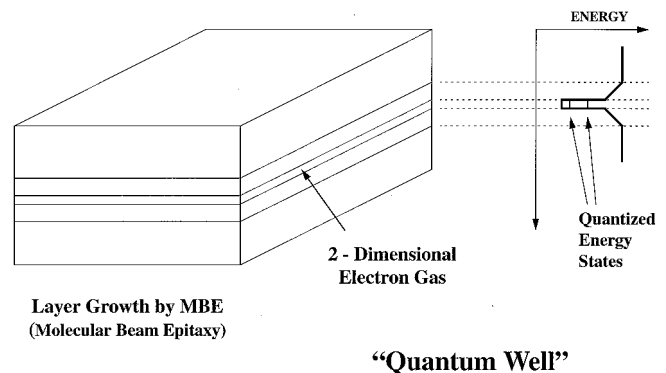


Fig. 4. Schematic diagram of a semiconductor sandwich structure with a “quantum well” layer resulting in a quasi two-dimensional electronic system.

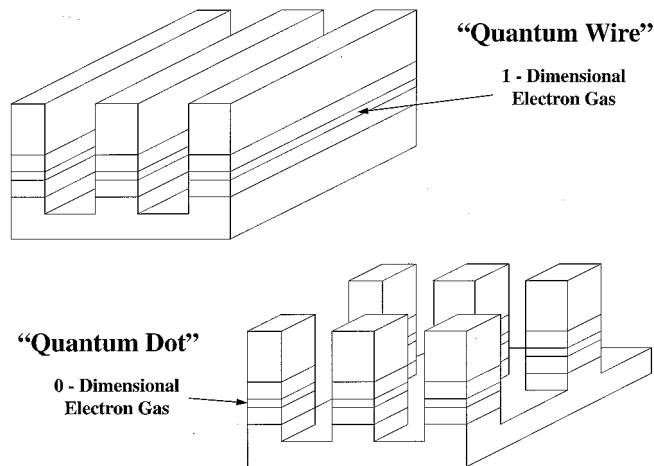


Fig. 5. Schematic diagram of etched lines resulting in “quantum wires” and etched pillars resulting in “quantum dots”.

electrons experience, as schematically shown in the figure. This technique is referred to as bandgap engineering and has been used extensively to tailor device structures [Capasso, 1990]. The layers can be grown sufficiently thin such that the quantum mechanical confinement effect becomes important. Also shown in the figure below are the resulting quantized energy states in the quantum well structure. This leads to the formation of a quasi two-dimensional electronic system in the quantum well layer (2DEG).

Control in the lateral direction can be achieved by conventional patterning techniques such as optical or electron-beam lithography. Subsequent processing steps, e.g. etching, can then selectively remove material to define lines or dot patterns, as schematically shown in Fig. 5. This processing results in further confinement of the 2DEG into quasi one-dimensional systems (so-called quantum wires) or even quasi zero-dimensional systems (so-called quantum dots) [Reed *et al.*, 1988; Meurer *et al.*, 1992].

A different approach of further constricting a 2DEG is to use electrostatic confinement. As schematically shown in Fig. 6, one may use lateral patterning techniques to shape a metallic layer which has been deposited onto the top surface of the MBE-grown semiconductor sandwich structure. Applying a negative bias to the gates will deplete the 2DEG underneath the metallic electrodes. In this fashion, one may create quantum wires by using two gates as schematically shown. In the literature, this technique is referred to as split-gate design [Thornton *et al.*, 1986]. Using a

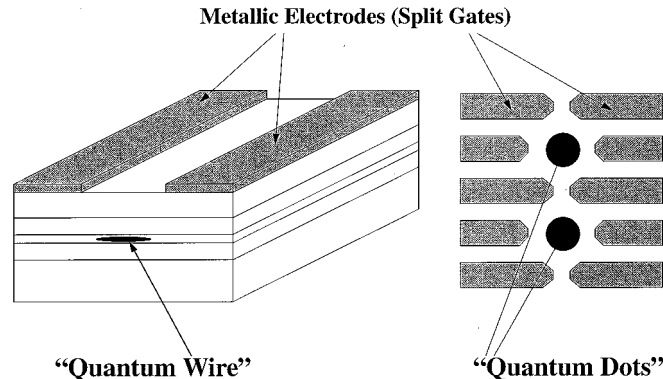


Fig. 6. Schematic diagram of further shaping a 2DEG into “quantum wires” and “quantum dots” by using electrostatic confinement provided by patterned metallic electrodes.

variety of gate structures, one may realize electronic systems of arbitrary shape. In particular, one may use gates to create “puddles” of electrons, thus realizing quantum dots [Meirav *et al.*, 1990]. In recent years, there have been a variety of experiments on such gate-confined quantum dots, and it has been demonstrated that the dot size, and thus also its occupation, can be adjusted by appropriately varying the bias voltages on the top gates [Hoffmann *et al.*, 1995; Waugh *et al.*, 1995; Blick *et al.*, 1996].

The techniques described so far utilize processing steps which are also used in conventional IC fabrication. In addition, more exotic nanostructure fabrication techniques are under study and development, which include the use of scanning tunneling microscope (STM) tips and chemical self-assembly.

Nanolithography using an atomic force microscope (AFM) is also possible. The atomically-sharp AFM tip may be used to either directly pattern the surface by scratching [Wendel *et al.*, 1996], or it may be used to induce local chemical or physical reaction thus modifying the surface [Lyding *et al.*, 1994]. AFM nanometer scale lithography has been described on various materials and structures, including processing at ambient conditions. The generated patterns can then be transferred to the two-dimensional electron gas by wet chemical etching or ion-beam irradiation.

Chemical self-assembly techniques may also be used to create nanostructure. Using special growth conditions, several groups have demonstrated that very thin semiconductor layers spontaneously assemble into tiny droplets, which exhibit quantum-confinement effects [Leonard *et al.*, 1993; Kirstaedter *et al.*, 1994; Temmyo *et al.*, 1995]. Elastic strain appears to play a critical role. While this

technique yields rather small dots (with sizes on the order of 10 nm, or so), the exact placement of these dots is still a problem, but progress is being made.

### 3. Quantum-Dot Cellular Automata

Based upon the emerging technology of quantum-dot fabrication, the Notre Dame NanoDevices group has proposed a scheme for computing with cells of coupled quantum dots [Lent *et al.*, 1993], which will be described below. To our knowledge, this is the first concrete proposal to utilize quantum dots for computing. There had been earlier suggestions that device-device coupling might be utilized in a cellular-automata scheme, but alas, these were without an accompanying proposal for a specific implementation [Ferry & Porod, 1986; Grondin *et al.*, 1987].

What we have in mind is the general architecture shown in Fig. 7. The coupling between the cells is given by their physical interaction, and not by wires. The physical mechanisms available for interactions between nanoelectronic structures are the Coulomb interaction and quantum-mechanical tunneling.

#### 3.1. A quantum-dot cell

Our proposal is based on a cell which contains five quantum dots [Lent *et al.*, 1993], as schematically shown in Fig. 8(a). The quantum dots are shown as the open circles which represent the confining electronic potential. In the ideal case, each cell is occupied by two electrons, which are schematically shown as the solid dots. The electrons are allowed to “jump” between the individual quantum dots in a cell by the mechanism of quantum mechanical tunneling. Tunneling is possible on the nanometer scale when the electronic wavefunction sufficiently “leaks” out of the confining potential of each dot, and the rate of these jumps may be controlled during fabrication by the physical separation between neighboring dots.

This quantum-dot cell represents an interesting dynamical system. The two electrons experience their mutual Coulombic repulsion, yet they are constrained to occupy the quantum dots. If left alone, they will seek, by hopping between the dots, the configuration corresponding to the physical ground state of the cell. It is clear that the two electrons will tend to occupy different dots because of the

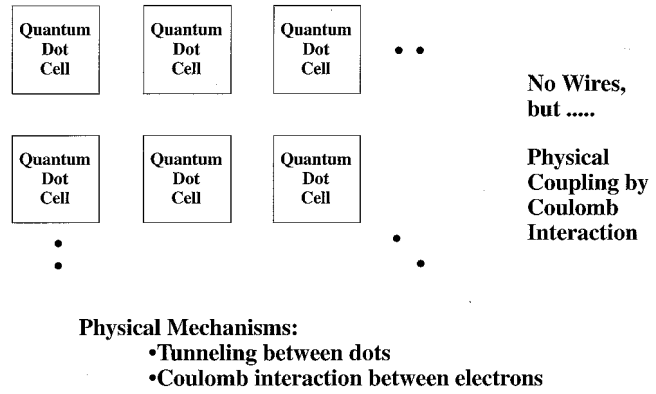


Fig. 7. Each cell in the array interacts with the “environment” which includes the Coulomb interaction with neighboring cells.

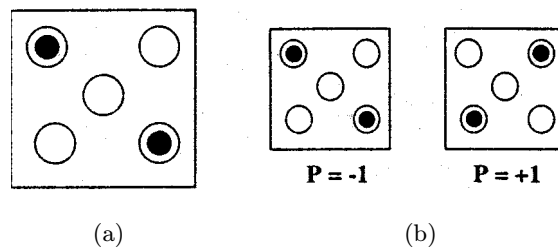


Fig. 8. (a) A quantum-dot cell consisting of five dots is occupied by two electrons. (b) The two distinct ground-state configurations with their respective polarizations.

Coulomb energy cost associated with bringing them together in close proximity on the same dot. It is easy to see that the ground state of the system will be an equal superposition of the two basic configurations with electrons at opposite corners, as shown in Fig. 8(b).

We may associate a “polarization” with a specific arrangement of the two electrons in each cell. Let us label the five dots in the following fashion: Starting from the upper right-hand corner, we label the dots in the four corners from 1 to 4, and the center dot as 0. We also denote the electron density in dot  $j$  by  $n_j$ , with the constraint that in each cell the sum of all the dot occupancies  $n_j$  has to add up to a total of 2 electrons. With that, we can define a cell polarization as

$$p = \frac{(n_1 + n_3) - (n_2 + n_4)}{n_0 + n_1 + n_2 + n_3 + n_4}$$

Note that this polarization is not a dipole moment, but a measure for the alignment of the charge along the two cell diagonals. A polarization of  $P = +1$  results if cells 1 and 3 are occupied, while electrons on sites 2 and 4 yield  $P = -1$  (compare Fig. 8).

Any polarization between these two extreme values is possible, corresponding to configurations where the electrons are more evenly “smeared out” over all dots. The ground state of an isolated cell is a superposition with equal weight of the two basic configurations, and therefore has a net polarization of zero.

As described in the literature, this cell has been studied by solving the Schrödinger equation using a quantum mechanical model Hamiltonian [Tougaw *et al.*, 1993]. We do not need to concern ourselves with the details here, suffice it to say that the basic ingredients to the equation of motion are: (1) the quantized energy levels in each dot, (2) the coupling between the dots by tunneling, (3) the Coulombic charge cost for a doubly-occupied dot, and (4) the Coulomb interaction between electrons in the same cell and also with those in neighboring cells. The solution of the Schrödinger equation, using cell parameters for an experimentally reasonable model, confirms the intuitive understanding that the ground state is a superposition of the  $P = +1$  and  $P = -1$  states. In addition to the ground state, the Hamiltonian model yields excited states and cell dynamics.

### 3.2. Cell-cell coupling

The properties of an isolated cell were discussed above. Here, we study the interactions between two cells, each consisting of five dots and each occupied by two electrons. The electrons are allowed to tunnel between the dots in the same cell, but not between different cells. Since the tunneling probabilities decay exponentially with distance, this can be achieved by having a larger dot-dot distance between cells, than within the same cell. Coupling between the two cells is provided by the Coulomb interaction between the electrons in different cells.

Figure 9 shows how one cell is influenced by the state of its neighbor. The inset shows two cells where the polarization of cell 1 ( $P_1$ ) is determined by the polarization of its neighbor ( $P_2$ ). The polarization of cell 2 is presumed to be fixed at a given value, corresponding to a certain arrangement of charges in cell 2, and this charge distribution exerts its influence on cell 1, thus determining its polarization  $P_1$ . The important finding here is the strongly nonlinear nature of the cell-cell coupling. As shown in the figure, cell 1 is almost completely polarized even though cell 2 might only be partially polarized. For example, a polarization of  $P_2 = 0.1$  induces

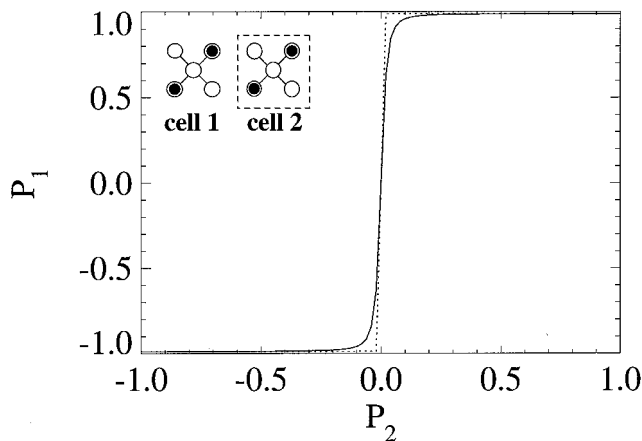


Fig. 9. Cell-cell coupling characteristic. Note the strongly nonlinear nature of the response which corresponds to “gain” in conventional devices.

almost perfect polarization in cell 1, i.e.  $P_1 = 0.99$ . In other words, even a small asymmetry of charge in cell 2 is sufficient to break the degeneracy of the two basic states in cell 1 by energetically favoring one configuration over the other.

The abruptness of the cell-cell response function depends upon the ratio of the strength of the tunneling energy to the Coulomb energy for electrons on neighboring sites. This reflects a competition between the kinetic and potential energy of the electron. For a large tunneling energy, an electron has a tendency to spread out more evenly over the available dots, and the nonlinearity becomes less pronounced. Stronger Coulomb coupling tends to keep electrons apart, and the nonlinearity becomes more pronounced. Properly designed cells will possess strongly nonlinear coupling characteristics.

This bistable saturation is the basis for the application of such quantum-dot cells for computing structures. The nonlinear saturation plays the role of gain in conventional circuits. Note that no power dissipation is required in this case. One can think of the saturation levels of the polarization as the “signal rails”.

These general conclusions regarding cell behavior and cell-cell coupling are not specific to the five-dot cell discussed so far. Similar behavior is also found for alternate cell designs, such as cells with only four dots in the corners, as opposed to the five discussed here [Tougaw *et al.*, 1993].

### 3.3. QCA logic

Based upon the bistable behavior of the cell-cell coupling, the cell polarization can be used to

encode binary information. We will show that the physical interactions between cells may be used to realize elementary Boolean logic functions [Lent *et al.*, 1994; Lent & Tougaw, 1994].

Figure 10 shows examples of simple cell arrays. In each case, the polarization of the cell at the edge of the array is kept fixed; this is the so-called driver cell and it is plotted with a thick border. We call it the driver since it determines the state of the whole array. Without a polarized driver, the cells in a given array would be unpolarized in the absence of a symmetry-breaking influence that would favor one of the basis states over the other. Each figure shows the cell polarizations corresponding to the physical ground state configuration of the whole array.

Figure 10(a) shows that a line of cells allows the propagation of information, thus realizing a binary wire. Note that only information but no electric current flows down the line, which results in low power dissipation. Information can also flow around corners, as shown in Fig. 10(b), and fan-out is possible, compare Fig. 10(c). A specific arrangement of cells, such as the one shown in Fig. 10(d), may be used to realize an inverter. In each case, electronic motion is confined to within a given cell, but not between different cells. Only information, and not charge, is allowed to propagate over the whole array.

These quantum-dot cells are an example of quantum-functional devices. Utilizing quantum-mechanical effects for device operation may give rise to new functionality. Figure 11 shows a majority logic gate, which simply consists of an intersection of lines and the “device cell” is just the one in the center. If we view three of the neighbors as inputs (kept fixed), then the polarization of the output cell is the one which “computes” the majority votes of the inputs. The figure also shows the majority logic truth table which was computed as the physical ground state polarizations for a given combination of inputs. Using conventional circuitry, the design of a majority logic gate would be significantly more complicated. The new physics of quantum mechanics gives rise to new functionality, which allows a rather compact realization of majority logic.

Note that conventional AND and OR gates are hidden in the majority logic gate. Inspection of the majority logic truth table reveals that if input A is kept fixed at 0, the remaining two inputs B and C realize an AND gate. Conversely, if A is held at 1, inputs B and C realize a binary OR gate. In other words, majority logic gates may be viewed as

programmable AND and OR gates, as schematically shown in Fig. 12. This opens up the interesting possibility that the functionality of the gate may be determined by the computation itself. The implications of this for circuit design and applications remain largely unexplored as of now.

One may conceive of larger arrays representing more complex logic functions. The largest structure simulated so far (containing some 200 cells) is a single-bit full adder, which may be designed by

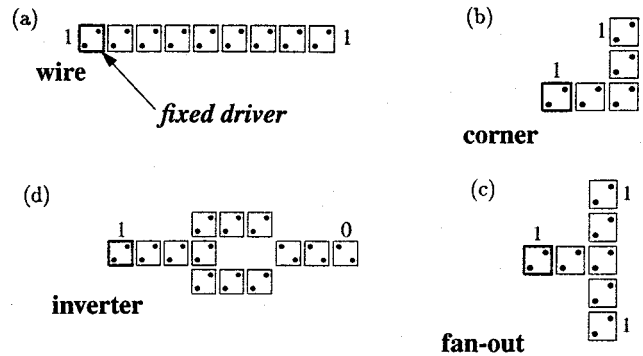


Fig. 10. Examples of simple QCA arrays showing (a) a binary wire, (b) signal propagation around corners, (c) the possibility of fan-out, and (d) an inverter.

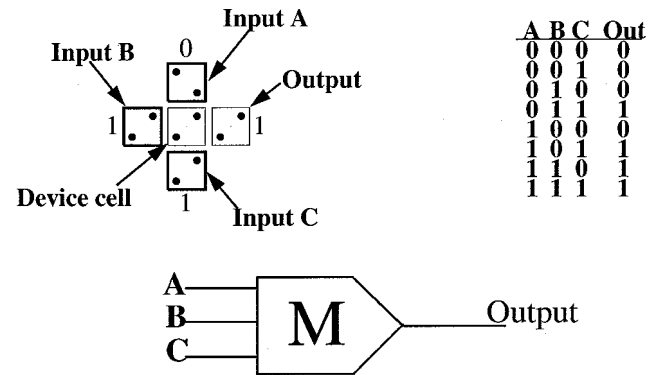


Fig. 11. Majority logic gate. The basic structure simply consists of an intersection of lines. Also shown are the computed majority logic truth table and its logic symbol.

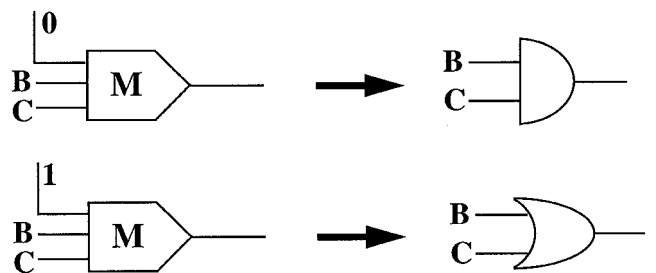


Fig. 12. Reduction of the majority logic gate to AND and OR gates by fixing one of the inputs.

taking advantage of the QCA majority logic gate as a primitive [Tougaw & Lent, 1994]. The general principles for computing with such QCA arrays will be discussed below.

### 3.4. Computing with QCA's

In a QCA array, cells interact with their neighbors, and neither power nor signal wires are brought to each cell. In contrast to conventional circuits, we do not have external control over each and every interior cell. Therefore, we need a new way of using such QCA arrays for computing. The main concept is that the information in a QCA array is contained in the physical ground state of the system. Figure 13 schematically illustrates the idea.

Computation in a QCA array proceeds along the following three basic steps:

- (i) First, the initial data is set by fixing the polarization of those cells at the edge, which represent the input information (edge-driven computation).
- (ii) Next, the whole array is allowed to relax (or is adiabatically transformed) to the new ground state, compatible with the input cells kept fixed (computing with the ground state).
- (iii) Finally, the results of the computation are read by sensing the polarization of those cells at the periphery which represent the output data.

The two key features which characterize this new computing paradigm are “computing with the

ground state” and “edge-driven computation” which we discuss in further detail below.

#### 3.4.1. Computing with the ground state

Consider a QCA array before the start of a computation. The array, left to itself, will have assumed its physical ground state. Presenting the input data, i.e. setting the polarization of the input cells, will deliver energy to the system, thus promoting the array to an excited state. The computation consists in the array reaching the new ground state configuration, compatible with the boundary conditions given by the fixed input cells. Note that the information is contained in the ground state itself, and not in how the ground state is reached. This relegates the question of the dynamics of the computation to one of secondary importance; although it is of significance, of course, for actual implementations. In the following, we will discuss two extreme cases for this dynamics, namely one where the system is completely left to itself, and another where exquisite external control is exercised.

*Let physics do the computing:* The natural tendency of a system to assume that the ground state may be used to drive the computation process. Dissipative processes due to the unavoidable coupling to the environment will relax the system from the initial excited state to the new ground state. The actual dynamics will be tremendously complicated since all the details of the system-environment coupling are unknown and uncontrollable. However, we do not have to concern ourselves with the detailed path in which the ground state is reached, as long as the ground state is reached. The attractive feature of this relaxation computation is that no external control is needed. However, there also are drawbacks in that the system may get “stuck” in metastable states and that there is no fixed time in which the computation is completed.

*Adiabatic computing:* Due to the above difficulties associated with metastable states, Lent and coworkers have developed a clocked adiabatic scheme for computing with QCA's. The system is always kept in its instantaneous ground state which is adiabatically transformed during the computation from the initial state to the desired final state. This is accomplished by lowering or raising potential barriers within the cells in concert with clock signals. The modulation of the potential barriers allows or inhibits changes of the cell

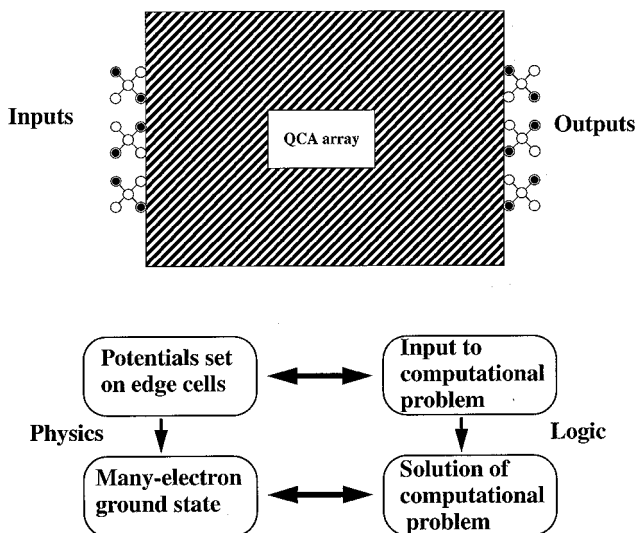


Fig. 13. Schematic representation of computing with a QCA array. The key concepts are “computing with the ground state” and “edge-driven computation” described in the text.

polarization. The presence of clocks makes synchronized operation possible, and pipelined architectures have been proposed [Lent *et al.*, 1994; Lent & Tougaw, 1997].

### 3.4.2. Edge-driven computation

Edge-driven computation means that only the periphery of a QCA array can be contacted, which is used to write the input data and to read the output of the computation. No internal cells may be contacted directly. This implies that no signals or power can be delivered from the outside to the interior of an array. All interior cells only interact within their local neighborhood. The absence of signal and power lines to each and every interior cell has obvious benefits for the interconnect problem and the heat dissipation.

The lack of direct contact to the interior cells also has profound consequences for the way such arrays can be used for computation. Since no power can flow from the outside, interior cells cannot be maintained in a far-from-equilibrium state. Since no external signals are brought to the inside, interior cells cannot be influenced directly. These are the reasons why the ground state of the whole array is used to represent the information, as opposed to the states of each individual cell. In fact, edge-driven computation necessitates computing with the ground state!

Conventional circuits, on the other hand, maintain devices in a far-from-equilibrium state. This has the advantage of noise immunity, but the price

to be paid comes in the form of the wires need to deliver the power (contributing to the wiring bottleneck) and the power dissipated during switching (contributing to the heat dissipation problem).

### 3.4.3. Thermodynamic considerations

Thermal fluctuations are of concern for ground state computing. Thermal noise may excite the system from its ground state to a higher-energy state, and thereby interfere with the computation. The probability for the occurrence of such errors is basically given by the relative magnitude of a typical excitation energy to the thermal energy,  $kT$ . Excitation energies become larger as the size of the system becomes smaller, thereby providing increasing noise immunity. A typical QCA cell fabricated with current state-of-the-art lithography (for minimum feature sizes of 20 nm) is expected to operate at cryogenic temperatures, whereas a molecular implementation (for feature sizes of 2 nm) would work at room temperature. This is illustrated in Fig. 14.

Thermodynamic considerations also are of concern for large arrays. Entropy needs to be taken into account. The tendency of a system to increase its entropy makes error states more favorable. As the size of the system increases, there are more and more error states. This sets an upper limit on the size of the allowed number of cells in an array before entropy takes over. It can be shown that this limit depends in an exponential fashion on the ratio of a typical excitation energy to the thermal energy

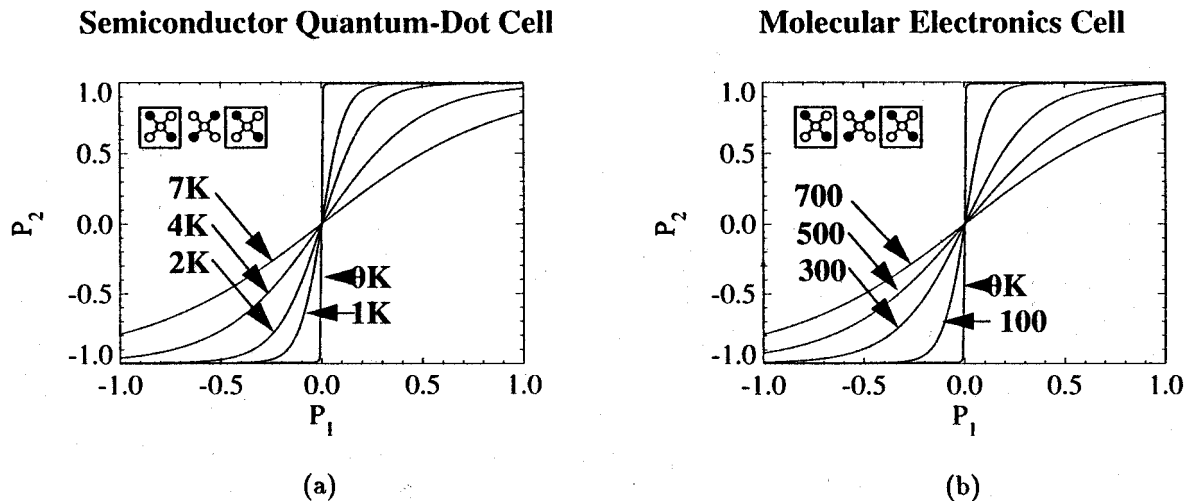


Fig. 14. Cell-cell response functions for various temperatures. (a) Semiconductor cell with minimum lithographic feature sizes of 20 nm and (b) molecular implementation with dimensions of 2 nm.

[Lent *et al.*, 1994]. For example, arrays with about 20,000 cells are feasible if this typical error energy is 10 times larger than the thermal energy.

### 3.5. Possible quantum-dot cell implementations

In this section, we discuss possible implementations of the coupled-quantum-dot cells discussed so far. Based upon the reported studies of dot-dot coupling in the literature, there is an experimental effort underway at Notre Dame to realize a cell using split-gate technology [Bernstein *et al.*, 1996]. We give a brief review of that work, including the results and implications of our numerical modeling. We also discuss a candidate molecule which might serve as a proto-type molecular electronics implementation of a QCA cell.

#### 3.5.1. Gate-controlled quantum dots

The fabrication of a QCA cell by split-gate technology is a challenging problem, yet appears to be within reach of current lithographic capability [Bernstein *et al.*, 1996]. Figure 15 shows a possible physical realization which is based on electrostatic confinement provided by a top metallic electrode. The key implementation challenges are (i) to gain sufficient gate control in order to define quantum dots in the few-electron regime, and (ii) to place these dots sufficiently close to each other in order to make coupling possible. Using these techniques, it is conceivable that coupled-dot cells may be realized in a variety of materials systems, such as III-V compound semiconductors, Si/SiGe heterolayers, and Si/SiO<sub>2</sub> structures.

In order to achieve a crisp confining potential, it is important to minimize the effects of fringing fields, which may be accomplished by bringing the electrons as close as possible to the top surface. This design strategy of “trading mobility versus gate control” by utilizing near-surface 2DEG’s has been pioneered by Snider, Hu and co-workers. However, the resultant proximity of the quan-

tum dot to the surface raises the question of the effect of the exposed surface on the quantum confinement. To study these questions, we have undertaken extensive numerical modeling of such gate-controlled dots, and we have explicitly included the influence of surface states which are occupied, in a self-consistent fashion, according to the local electrostatic potential [Chen & Porod, 1995].

We have performed numerical simulations for the design of quantum dot structures in the few-electron regime, both in the AlGaAs/GaAs and Si/SiO<sub>2</sub> material systems. The confining potential is obtained from the Poisson equation within a Thomas-Fermi charge model. The electronic states in the quantum dot are then obtained from solutions of the axisymmetric Schrödinger equation.

Our model takes into account the effect of surface states by viewing the exposed surface as the interface between the semiconductor and air (or vacuum). Figure 16 schematically shows the simulation strategy, where we employ a finite-element technique for the semiconductor domain and a boundary element method for the dielectric above [Chen *et al.*, 1994]. Both domains are coupled at the exposed surface, taking into account the effect of charged surface states. This is particularly important for modeling the III-V material system, where surface states are known to be significant.

Our modeling shows that the single most critical parameter for the design of gate-controlled dots is the proximity of the 2DEG to the top metallic gates. This distance is limited in the III-V material system by the “leakyness” of the layer separating the electronic system from the electrodes. Distances as close as 25 nm have been achieved, but more typically 40 nm are being used. The silicon material system appears to be a particularly promising candidate because of the extremely good insulating properties of its native oxide. SiO<sub>2</sub> layers can be made as thin as 10 nm, and even less (4 nm appears to be about the limit). This allows for extremely crisp confining potentials.

We have explored various gate configurations and biasing modes. Our simulations show that the

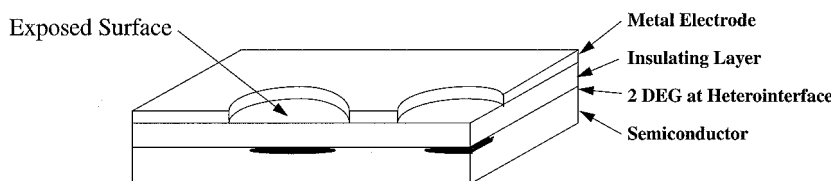


Fig. 15. Possible physical realization of gate-controlled quantum dots by top metallic gates.

number of electrons can be effectively controlled in the few electron regime by the combined action of depletion and enhancement gates, which we will illustrate below.

3.5.2. *AlGaAs/GaAs material system*

Figure 17 shows an example of the occupation of quantum dots for combined enhancement/depletion mode biasing on an AlGaAs/GaAs 2DEG. The main idea is to negatively bias the outer electrode (gate 2) such that the 2D electron density is depleted, or near depletion; a positive bias on the inner electrode (gate 1) is then utilized to induce the quantum dot and to control its occupation. In this

example, we have chosen a radius of  $r_{G1} = 6 \text{ nm}$  for the center enhancement gate, and a radius of  $r_{G2} = 50 \text{ nm}$  for the surrounding depletion gate. The resulting number of electrons induced by three different voltages on the depletion gate,  $V_{G2}$ , is plotted as a function of the enhancement gate bias voltage,  $V_{G1}$ . We see that variations of the depletion-gate bias of 10 mV will result in threshold-voltage variations of as much as 80 mV. This biasing mode appears to be an effective way of controlling the quantum-dot threshold voltage in the few-electron regime.

The use of a single, negatively-biased depletion gate would not suffice for our purposes. Even though it would be possible to obtain

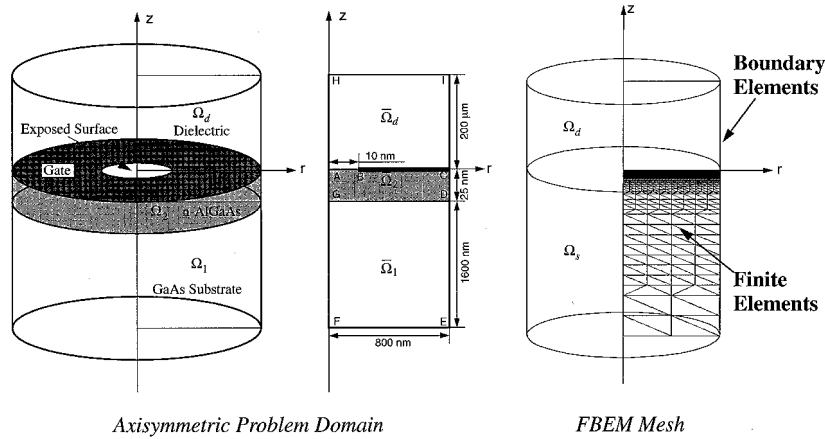


Fig. 16. Solution strategy used in the numerical simulations. Finite elements are used in the semiconductor domain, and a boundary element technique for the dielectric above.

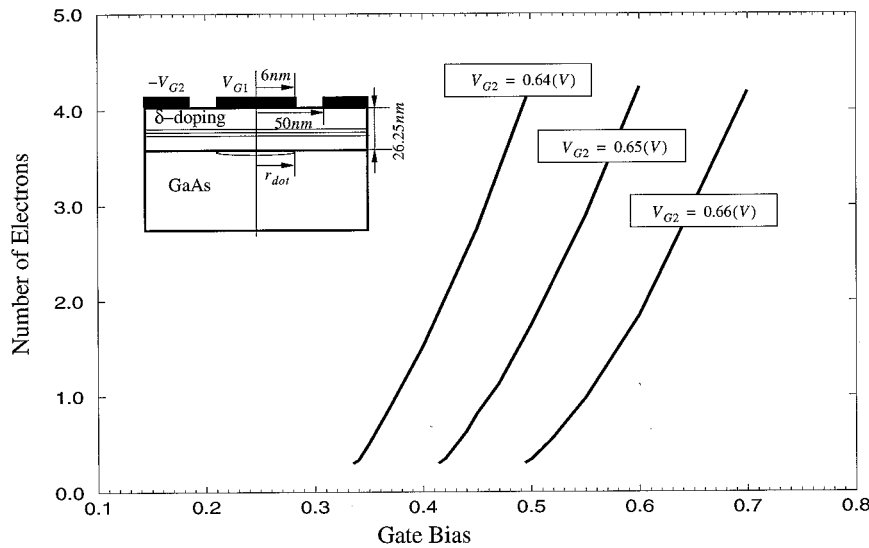


Fig. 17. Example of dot occupation using combined enhancement (G1) and depletion (G2) gates in the AlGaAs/GaAs material system.

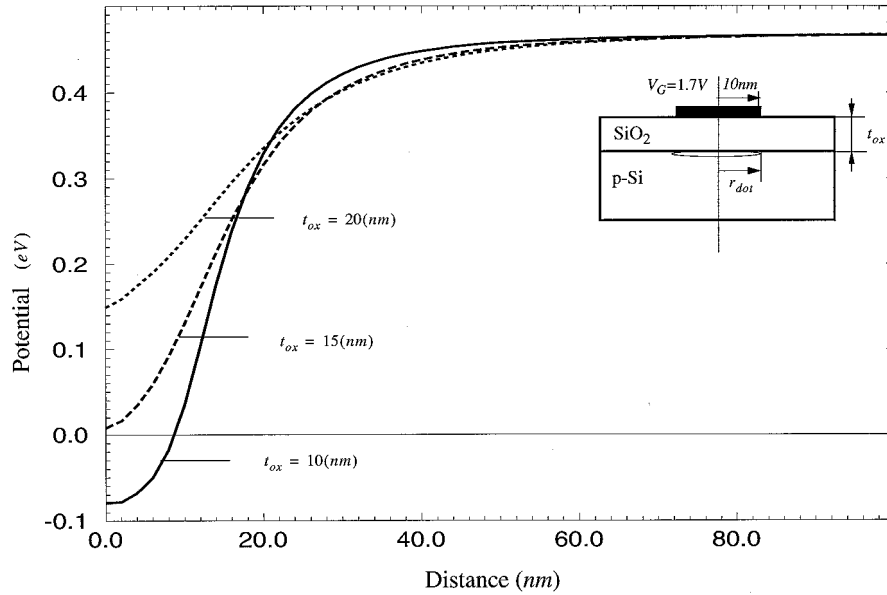


Fig. 18. Potential variation at the silicon/silicon dioxide interface as a function of oxide thickness.

few-electron dots, the resulting potential variations are too gradual to allow fabrication of a QCA cell with closely-spaced dots [Chen & Porod, 1995].

### 3.5.3. *Si/SiO<sub>2</sub> material system*

We have also performed numerical simulations for the design of gated few-electron quantum dot structures in the Si/SiO<sub>2</sub> material system. The motivation for this work has been to investigate the feasibility of transferring the emerging technology of quantum dot fabrication from the III-V semiconductors, where it was pioneered over the past few years, to the technologically more important Si/SiO<sub>2</sub> material system. Silicon appears to be a promising candidate due to the excellent insulating behavior of thin SiO<sub>2</sub> films which yields the required crisp gate-control of the potential in the plane of the two-dimensional electron gas at the Si/SiO<sub>2</sub> interface. Another advantage of silicon for quantum dot applications appears to be the higher effective mass, as compared to the III-V materials, which reduces the sensitivity of the energy levels to size fluctuations.

Quantum dots may be realized by applying a positive bias to a metallic gate on the surface, as schematically shown in the inset to Fig. 18. The positive voltage induces an inversion layer underneath the biased gate, which may lead to the formation of an “electron droplet” at the silicon/oxide interface, i.e. a quantum dot. Figure 18 shows, for an applied gate bias of 1.7 V, the corresponding po-

tential variations along the Si/SiO<sub>2</sub> interface. An electronic system is induced when the silicon conduction band edge at the oxide interface, indicated by the solid line, dips below the Fermi level (indicated by the thin horizontal line). We see that the formation of a quantum dot critically depends upon the thickness of the oxide layer. Our modeling shows that for a 10 nm gate radius, an oxide thickness around (or below) 10 nm is required. Further modeling shows that these dots are occupied in the few-electron regime [Chen & Porod, 1996].

Our modeling suggests a design strategy as schematically shown in Fig. 19. Two metallic electrodes are being used, one (the bottom one) as a depletion gate, and the top one as an enhancement gate. We envision to fabricate openings

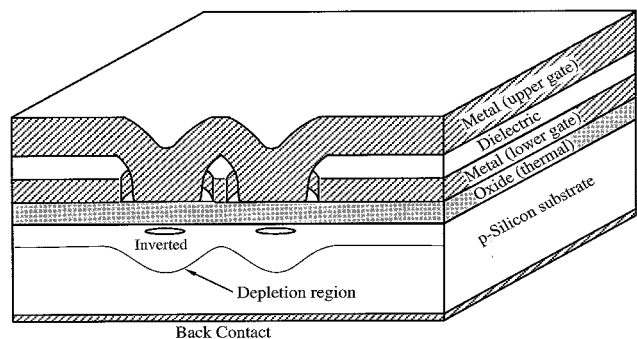


Fig. 19. Design strategy for a quantum-dot cell in the silicon material system using the combined action of two metallic electrodes.

in the bottom electrode by electron beam lithography with dimensions of about 20 nm. The top electrode is then evaporated onto the patterned and oxidized metallic layer, which results in a top electrode which may reach the semiconductor surface inside the openings, providing the enhancement gates.

### 3.5.4. Rings of metallic tunnel junctions

In addition to the semiconductor systems discussed above, single-electron tunneling phenomena may also be observed in metallic tunnel junctions [Grabert & Devoret, 1992]. It is possible to fabricate tiny metallic droplets with self-capacitances on the order of atto-Farads ( $10^{-18}$  F). Adding (or subtracting) a single electron to (or from) such a miniscule metallic particle, will result in easily observable voltage variations on the order of 1/10th

of 1 Volt! This is the basic idea behind the phenomenon of “Coulomb blockade”.

Consider a ring of metallic tunnel junctions, schematically shown in Fig. 20(a). The tunnel junctions are represented by the crossed capacitor symbols, indicating that these junctions are characterized by their capacitance and tunnel resistance. The metallic droplets themselves are the “wires” between the tunnel junctions. Consider now that two extra electrons are added to such a cell, as schematically shown in part (b) of the figure. It can be shown that this cell exhibits precisely the same two distinct ground state configurations as the semiconductor cell discussed above. In addition, the cell-cell coupling also shows the same strongly nonlinear saturating characteristic [Lent & Tougaw, 1994]. Note that cell-cell coupling is purely capacitive, as schematically shown for the line of cells in Fig. 20(c). The metallic tunnel junction cell may

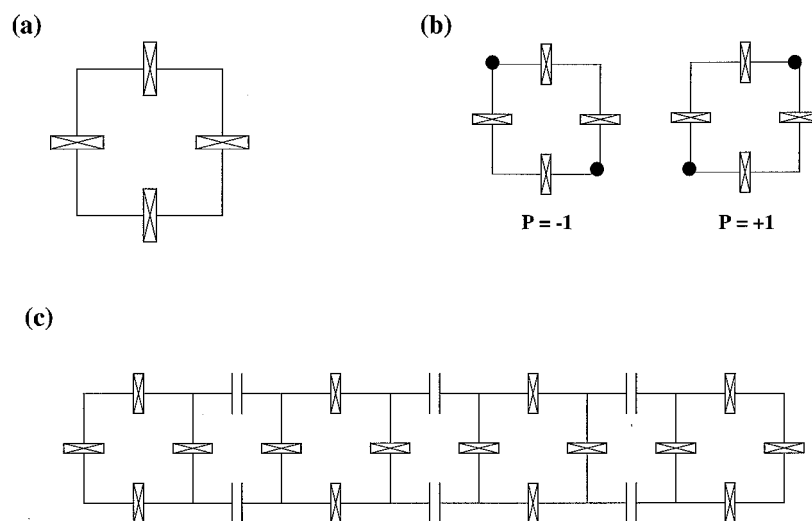


Fig. 20. Possible QCA implementation using rings of metallic tunnel junctions. (a) Basic cell, (b) cell occupied by two additional electrons, (c) line of capacitively coupled cells.

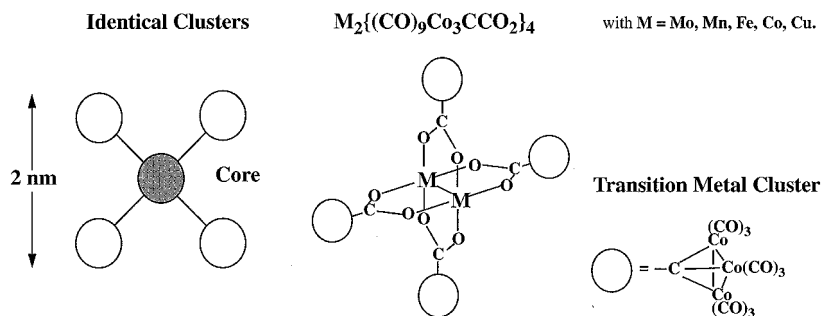


Fig. 21. Candidate for a molecular QCA cell consisting of four outer  $(CO)_9Co_3C$  clusters which are arranged in a plane around a “spindle” constituted by the  $M_2$  core.

be used as a building block for more complicated structures, in a fashion completely analogous to the semiconductor implementations.

Using the technique of shadow evaporation, coupled-dot structures have recently been fabricated and tested in the aluminum–aluminum oxide material system [Bernstein & Snider, 1996]. To date, a coupled two-dot system has been investigated and the charge state of each dot could be measured independently. Work on a four-dot ring of tunnel junctions is in progress.

### 3.5.5. Possible molecular implementation

As discussed above, QCA room temperature operation would require molecular-scale implementations of the basic cell. Molecular chemistry promises to offer the versatility for the desired miniaturization.

The requirements for a molecular QCA technology include: (1) Cells made of a rigid array of identical clusters with inter-cell interactions that are insulating (e.g. a square arrangement of four clusters); (2) Two-electron occupation of each cell with distinct arrangements of the two charges; (3) Charge interchange between these distinct arrangements, which are energetically equal in the absence of a polarizing field; (4) Patterning of cells into predefined array geometries on a substrate; (5) Connections to the periphery of an array for inputs and outputs.

In previous work by Fehlner and co-workers, a candidate for such a prototypical molecular cell had been synthesized and crystallographically characterized [Cen *et al.*, 1992]. As schematically illustrated in Fig. 21, these molecular substances with the formula  $M_2\{(CO)_9Co_3CCO_2\}_4$ , where  $M=Mo, Mn, Fe, Co, Cu$ , consist of square arrays of transition metal clusters, each containing three cobalt atoms. It is remarkable that the four clusters are arranged in a (flat) square, as opposed to a (three-dimensional) tetrahedron, which one might have expected. The reason for this behavior lies in the two metallic atoms at the center which form a “spindle” and the clusters attach themselves in the plane perpendicular to this axis.

It has been demonstrated that these compounds may be obtained as pure crystalline molecular solids in gram quantities. In spite of high molecular weights, these substances are soluble and most dissolve without dissociation, which makes it possible to disperse them on a substrate. Each cell has an edge-to-edge distance of about 2 nm, which is precisely the desired dimension for QCA room

temperature operation. The spectroscopic properties demonstrate intra-cell cluster-core electronic communication and inter-cell interactions are insulating.

## 4. Quantum-Dot Cellular Neural Networks

In addition to employing QCA cells to encode binary information, these cells may also be used in an analog mode. As schematically shown in Fig. 22, each cell interacts with its neighbors within a certain range, thus forming what we call a *Quantum-Dot Cellular Nonlinear Network* (Q-CNN) [Toth *et al.*, 1996]. This way of viewing coupled cells as a nonlinear dynamical system is similar to *Cellular Nonlinear (or, Neural) Networks* (CNN), which are locally-interconnected structures implemented using conventional circuitry [Chua & Yang, 1988a, 1988b]. Each cell is described by appropriate state variables, and the dynamics of the whole array is given by the dynamical law for each cell, which includes the influence exerted by the neighbors on any given cell.

In the paragraphs below, we develop a simple two-state model for the quantum states in each cell and show how the quantum dynamics of the array can be transformed into a CNN-style description by choosing appropriate state variables. The general features of this model are: (1) Each cell is a quantum system, characterized by both classical and quantum degrees of freedom. (2) The interactions between cells only depends upon the classical degrees of freedom; the precise form of the

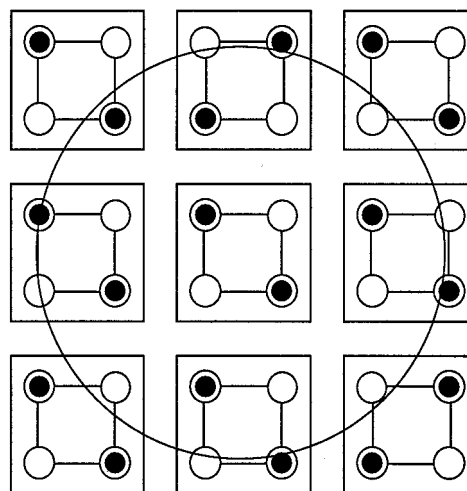


Fig. 22. Schematic view of a locally-connected cellular QCA array. The circle indicates the range of interaction for the central cell.

“synaptic input” is determined by the physics of the intercellular interactions. (3) The state equations are derived from the time-dependent Schrödinger equation; one state equation exists for each classical and quantum degree of freedom.

For the case of a two-dimensional array, each Q-CNN cell possesses an equivalent CNN-cell model described by the differential equations given below. We may thus think of such a quantum-dot cell array as a special case of cellular nonlinear networks [Nossek & Roska, 1993]. The equivalent circuit describing a cell is composed of two linear capacitors, four nonlinear controlled sources and eight linear controlled sources representing the interactions between the cell and its eight neighbors [Csurgay, 1996].

Our quantum model is a special case of a general formalism for “quantum networks” developed by Mahler [1995]. As schematically shown in Fig. 23, a quantum network consists of subsystems which are special quantum objects denoted as “network nodes” and the interaction channels between them are denoted as “network edges”. In his book, Mahler develops the theoretical study of small (coherent) quantum networks by means of the density matrix theory: the network node is taken as a finite local state space of dimension  $n$ . The network might be a regular lattice or an irregular array of nodes. The network is coupled to external driving fields and dissipative channels, which are required for measurement. This approach provides a system-theoretic tool adaptable to situations where a finite quantum mechanical state space is controlled by a classical environment. In other words, this formalism also includes dissipation, which we have not yet incorporated in our Q-CNN model, but this work is in progress.

### 4.1. Quantum model of cell array

Following the work of Toth *et al.* [1996], we describe the quantum state in each cell using the two basis states  $|\phi_1\rangle$  and  $|\phi_2\rangle$  which are completely polarized.

$$|\Psi\rangle = \alpha|\phi_1\rangle + \beta|\phi_2\rangle$$

Within this two-state model, each property of a cell is completely specified by the quantum mechanical amplitudes  $\alpha$  and  $\beta$ . In particular,  $P$ , the cell polarization is given by:

$$P = |\alpha|^2 - |\beta|^2$$

The Coulomb interaction between adjacent cells increases the energy of the configuration if the two

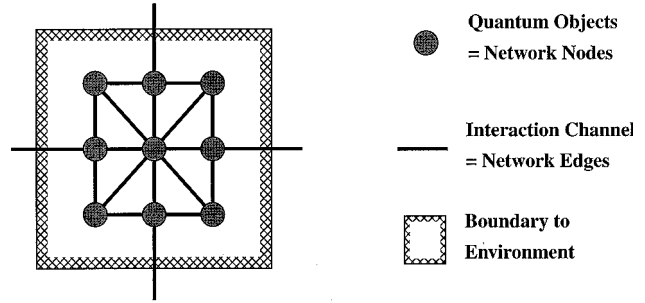


Fig. 23. Quantum Network: the subsystems of the network are special quantum objects denoted as “network nodes” and the interaction channels are denoted as “network edges” (after [Mahler, 1995]).

cell polarizations differ. This can be accounted for by an energy shift corresponding to the weighted sum of the neighboring polarizations, which we denote by  $\overline{PE}$ . The cell dynamics is then given by the Schrödinger equation,

$$i\hbar\delta/\delta t|\Psi\rangle = H|\Psi\rangle$$

where  $H$  represents the cell Hamiltonian. Once the Hamiltonian is specified, the cell dynamics is completely determined. Since  $|\Psi\rangle$  represents the state of a given cell, and not the state of the whole array, quantum entanglement is not accounted for in this formulation.

### 4.2. Formulating CNN-like quantum dynamics

In order to transform the quantum mechanical description of an array into a CNN-style description, we perform a transformation from the quantum-mechanical state variables to a set of state variables which contains the classical cell polarization,  $P$ , and a quantum mechanical phase angle,  $\varphi$ :

$$|\Psi\rangle = (\alpha, \beta) \longrightarrow |\Psi\rangle = (P, \varphi)$$

This transformation is accomplished by the following relations:

$$\alpha = ((1 + P)/2)^{1/2}$$

$$\beta = ((1 - P)/2)^{1/2} e^{i\varphi}$$

With this, the dynamical equations derived from the Schrödinger can be rewritten as CNN-like dynamical equations for the new state variables  $P$  and  $\varphi$

$$\hbar\delta/\delta tP = -2\gamma \sin \varphi(1 - P^2)^{1/2}$$

$$\hbar\delta/\delta t\varphi = -\overline{PE} + 2\gamma \cos \varphi P/(1 - P^2)^{1/2}$$

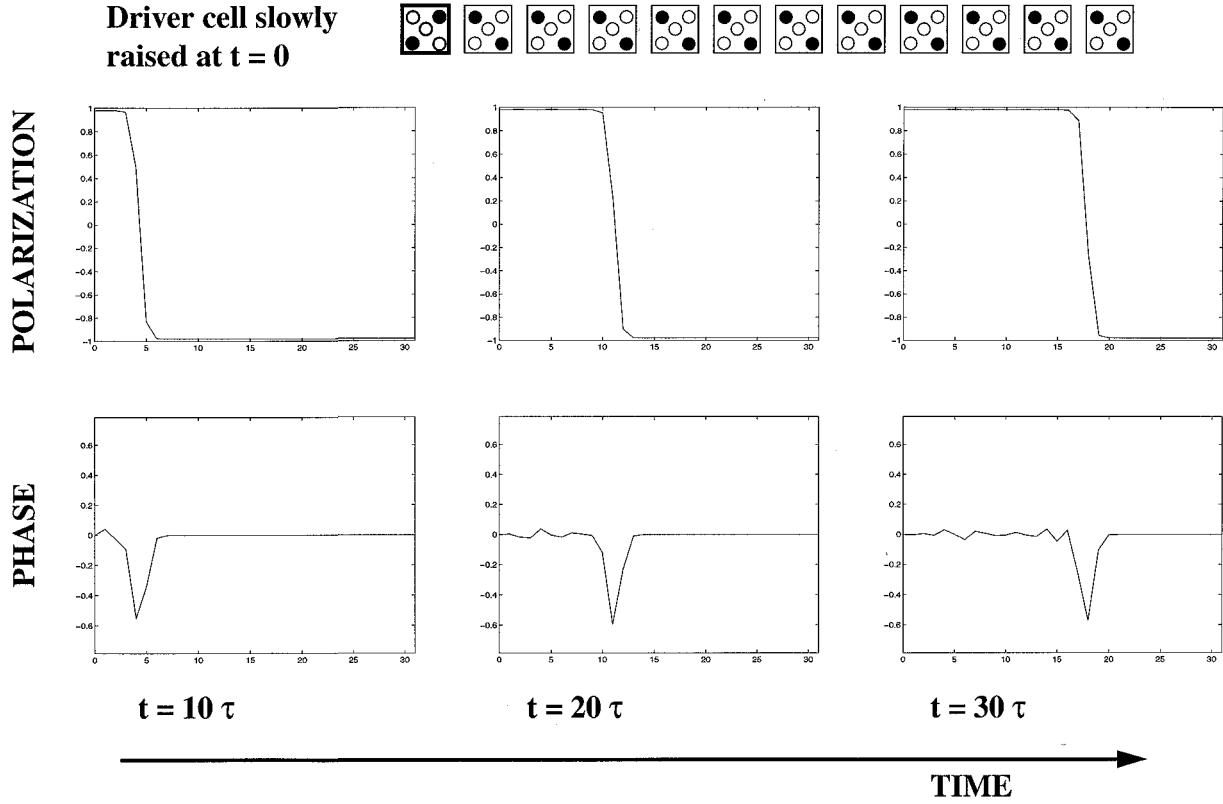


Fig. 24. Wave front motion in a linear Q-CNN array.

The term  $\overline{PE}$  accounts for the cell-cell interaction and  $\gamma$  is the tunneling matrix element between dots. For a more detailed derivation, we refer to the original paper by Toth and co-workers [1996].

It can be shown that the resulting dynamics for each cell is governed by a Liapounov function  $V(P, \varphi)$  which is given by:

$$V(P, \varphi) = 2\gamma \cos \varphi (1 - P^2)^{1/2} + P\overline{PE}$$

### 4.3. Cellular network model of quantum-dot array

This above network model simulates the dynamics of the polarization and the phase of the coupled cellular array. If the polarization of the driver cells of an array in equilibrium is changed in time, a dynamics of the polarizations and phases for all cells in the whole array is launched. In the framework of the CNN model, ground-state computing by the Quantum Cellular Array corresponds to transients between equilibrium states.

It is well known for CNN arrays that the dynamics may give rise to interesting spatio-temporal wave-phenomena [Chua, 1995]. A significant literature exists on this subject, and different classes

of wave behavior and pattern formation have been identified.

By complete analogy, spatio-temporal wave behavior also exists for the dynamics of Q-CNN arrays. We have begun to study these phenomena, and we present a few examples below.

Figure 24 shows wave front motion in a linear Q-CNN array. The driver cell on the left-hand-side is switched at  $t = 0$ , thereby launching such a soliton-like wave front. The figure shows snapshots of the classical polarization  $P$  and the quantum mechanical phase angle  $\varphi$  at various times. Note that the information about the direction of propagation is contained in the sign of the phase angle. Just from the polarization alone, one could not tell whether the wave front would move to the right or left.

Figure 25 shows examples of wave-like excitation patterns in two-dimensional Q-CNN arrays. The top panel shows an example of wave behavior induced by a periodic modulation of the boundaries. Note that a fixed cell block is also included near the upper left-hand corner. Several snapshots are shown (time increases from left to right) which display concentric wave fronts. The bottom panel shows an example of cyclical excitations at the boundaries which give rise to a spiral wave.

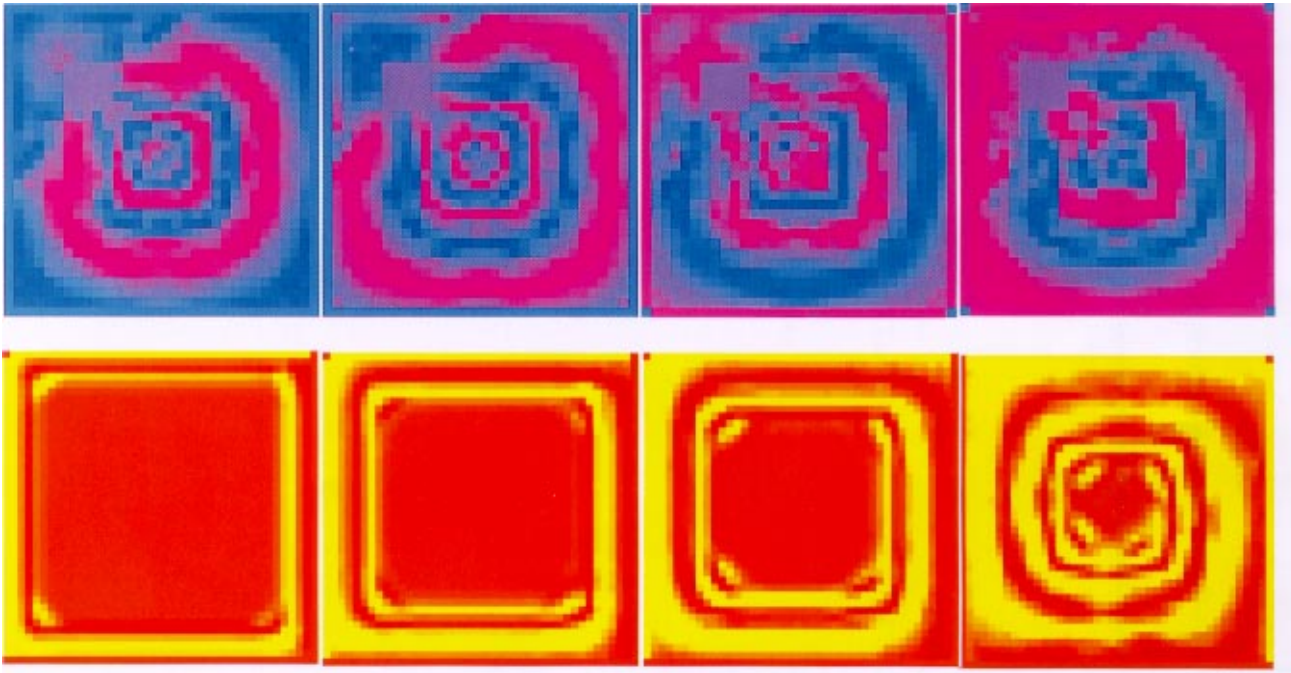


Fig. 25. Examples of wave-like excitation patterns in two-dimensional Q-CNN arrays. The top panel shows concentric waves due to a periodic modulation of the boundaries. The bottom panel shows a spiral wave due to cyclical modulation of the boundaries.

The excitation at each of the four boundaries are 90 degrees out of phase with respect to their neighboring edge.

## Acknowledgments

The work reviewed in this paper represents the collective effort of the Notre Dame NanoDevices Group, specifically Profs. Craig Lent, Gary Bernstein, Greg Snider, and Jim Merz. On the systems aspects of this work, I gratefully acknowledge my collaborators Profs. Arpad Csurgay, Yih-Fang Huang, and Ruey-Wen Liu. Special thanks go to Geza Toth for help with figures, and Prof. Arpad Csurgay for many helpful comments and a critical reading of the manuscript.

## References

- Ashoori, R. C. [1996] "Electrons in artificial atoms," *Nature* **379**, 413.
- Bernstein, G. H., Bazan, G., Chen, M., Lent, C. S., Merz, J. L., Orlov, A. O., Porod, W., Snider, G. L. & Tougaw, P. D. [1996] "Practical issues in the realization of quantum-dot cellular automata," *Superlatt. Microstruct.* **20**, 447–459.
- Bernstein, G. H. & Snider, G. L. [1996] private communication.
- Biafore, M. [1994] "Cellular automata for nanometer-scale computation," *Physica* **D70**, 415.
- Blick, R. H., Haug, R. J., Weis, J., Pfannkuche, D., Klitzing, K. V. & Eberl, K. [1996] "Single-electron tunneling through a double quantum dot: The artificial molecule," *Phys. Rev.* **B53**, 7899–7902.
- Capasso, F. (ed.) [1990] *Physics of Quantum Electron Devices*, Springer Series in Electronics and Photonics **28** (Springer-Verlag, Berlin Heidelberg).
- Cen, W., Lindenfeld, P. & Fehlner, T. P. [1992] "On the interface of metal-metal multiple bond compounds and organometallic clusters," *J. Am. Chem. Soc.* **114**, 5451–5452.
- Chen, M., Porod, W. & Kirkner, D. J. [1994] "A coupled finite element/boundary element method for semiconductor quantum devices with exposed surfaces," *J. Appl. Phys.* **75**, 2545–2554.
- Chen, M. & Porod, W. [1995] "Design of gate-confined quantum dot structures in the few-electron regime," *J. Appl. Phys.* **78**, 1050–1057.
- Chen, M. & Porod, W. [1996] "Simulation of quantum-dot structures in Si/SiO<sub>2</sub>," *VLSI Design* in press.
- Chua, L. O. & Yang, L. [1988a] "Cellular neural networks: Theory," *IEEE Trans. Circuits Syst.* **CAS-35**, 1257–1272.
- Chua, L. O. & Yang, L. [1988b] "CNN: Applications," *IEEE Trans. Circuits Syst.* **CAS-35**, 1273–1290.
- Chua, L. O. (ed.) [1995] *Special Issue on Nonlinear Waves, Patterns and Spatio-Temporal Chaos in Dynamic Arrays*, *IEEE Trans. Circuits Syst., I. Fundamental Theory and Applications* **42**(10), (October issue).

- Csurgay, A. [1996] private communication.
- Esaki, L. & Tsu, R. [1970] "Superlattice and negative differential conductivity in semiconductors," *IBM J. Res. Develop.* **14**, 61.
- Ferry, D. K. & Porod, W. [1986] "Interconnections and architecture for ensembles of microstructures," *Superlatt. Microstruct.* **2**, 41.
- Ferry, D. K., Grondin, R. O. & Porod, W. [1987] "Interconnection, dissipation, and computation," in *VLSI Electronics: Microstructure Science*, Vol. 15, eds. Einspruch, N. G., Cohen, S. S. & Gildenblat, G. (Academic Press), p. 451.
- Frisch, U., Hasslacher, B. & Pomeau, Y. [1986] "Lattice-gas automata for the Navier–Stokes equation," *Phys. Rev. Lett.* **56**, 1505–1508.
- Grabert, H. & Devoret, M. H. (eds.) [1992] *Single Charge Tunneling* (Plenum, New York).
- Grondin, R. O., Porod, W., Loeffler, C. M. & Ferry, D. K. [1987] "Cooperative effects in interconnected device arrays," in *Molecular Electronic Devices II* ed. Carter, F. L. (Dekker), pp. 605–622.
- Ferry, D. K., Akers, L. A. & Greeneich [1988] *Ultra Large Scale Integrated Microelectronics* (Prentice Hall).
- Hoffmann, F., Heinzl, T., Wharam, D. A., Kotthaus, J. P., Böhm, G., Klein, W., Tränkle, G. & Weimann, G. [1995] "Single electron switching in a parallel quantum dot," *Phys. Rev.* **B51**, 13872–13875.
- Kastner, M. A. [1993] "Artificial atoms," *Physics Today* **46**, 24.
- Kelly, M. J. [1995] *Low-Dimensional Semiconductors: Materials, Physics, Technology, Devices* (Oxford Science Publications).
- Keyes, R. W. [1987] *The Physics of VLSI Systems* (Addison-Wesley).
- Kirstaedter, N., Ledentsov, N. N., Grundman, M., Bimberg, D., Ustinov, V. M., Ruminov, S. S., Maximov, M. V., Kop'ev, P. S. & Alferov, Zh. I. [1994] "Low threshold, large  $T_0$  injection laser emission from (InGa)As quantum dots," *Electron. Lett.* **30**, 1416–1417.
- Lent, C. S., Tougaw, P. D., Porod, W. & Bernstein, G. H. [1993] "Quantum cellular automata," *Nanotechnology* **4**, 49–57.
- Lent, C. S., Tougaw, P. D. & Porod, W. [1993] "Bistable saturation in coupled quantum dots for quantum cellular automata," *Appl. Phys. Lett.* **62**, 714–716.
- Lent, C. S. & Tougaw, P. D. [1994] "Bistable saturation due to single electron charging in rings of tunnel junction," *J. Appl. Phys.* **75**, 4077–4080.
- Lent, C. S., Tougaw, P. D. & Porod, W. [1994] "Quantum cellular automata: The physics of computing with arrays of quantum-dot molecules," in *Proc. Workshop on Physics and Computation, PhysComp94* (IEEE Computer Society Press), pp. 1–9.
- Lent, C. S. & Tougaw, P. D. [1997] "A device architecture for computing with quantum dots," *Proc. IEEE Aprre 97* Vol. 85, No. 4, pp. 541–557.
- Leonhard, D., Krishnamurty, M., Reaves, C., Denbaars, S. & Petroff, P. [1993] "Direct formation of quantum-sized dots from uniform coherent islands of InGaAs on GaAs surfaces," *Appl. Phys. Lett.* **63**, 3203–3205.
- Lyding, J. W., Shen, T.-C., Hubacek, J. S., Tucker, J. R. & Abeln, G. C. [1994] "Nanoscale patterning and oxidation of H-passivated Si(100)– $2 \times 1$  surfaces with an ultrahigh vacuum scanning tunneling microscope," *Appl. Phys. Lett.* **64**, 2010–2012.
- Mahler, G. & Weberruß, V. A. [1995] *Quantum Networks: Dynamics of Open Nanostructures* (Springer-Verlag, Berlin Heidelberg).
- Meirav, U., Kastner, M. A. & Wind, S. J. [1990] "Single-electron charging and periodic conductance resonances in GaAs nanostructures," *Phys. Rev. Lett.* **65**, 771–774.
- Meurer, B., Heitmann, D. & Ploog, K. [1992] "Single-electron charging of quantum-dot atoms," *Phys. Rev. Lett.* **68**, 1371–1374.
- Montemerlo, M. S., Love, C. J., Opiteck, G. J., Goldhaber-Gordon, D. & Ellenbogen, J. C. [1996], "Technologies and designs for electronic nanocomputers," The MITRE Corp. preprint available from <http://www.mitre.org/research/nanotech/>.
- Nossek, J. A. & Roska, T. [1993] *Special Issue on Cellular Neural Networks, IEEE Trans. Circuits Syst., I. Fundamental Theory and Applications*, **40**(3).
- Porod, W., Harbury, H. K. & Lent, C. S. [1996] "Study of wave phenomena in physically-coupled device arrays using the Helmholtz equation as a model," presented at the *Fourth Workshop on Physics and Computation — PhysComp96*.
- Reed, M. A., Randall, J. N., Aggarwal, R. J., Matyi, R. J., Moore, T. M. & Wetsel, A. E. [1988] "Observation of discrete electronic states in zero-dimensional semiconductor nanostructures," *Phys. Rev. Lett.* **60**, 535–538.
- Semiconductor Industry Association [1994] *The National Technology Roadmap for Semiconductors*, Sematech, Austin TX.
- Spiller, T. P. [1996] "Quantum information processing: Cryptography, computation, and teleportation," in *Proc. IEEE* **84**, 1719–1746.
- Temmyo, J., Kuramochi, E., Sugo, M., Nishiya, T., Notzel, R. & Tamamura, T. [1995] "Quantum disc laser with self-organized dot-like active regions," *Proc. Lasers and Electro-Optic Society* **1**, 77–78.
- Thornton, T. J., Pepper, M., Ahmed, H., Andrews, D. & Davies, G. J. [1986] "One-dimensional conduction in the 2-d electron gas," *Phys. Rev. Lett.* **56**, 1198–1201.
- Toffoli, T. & Margolus, N. [1987] *Cellular Automata Machines: A New Environment for Modeling* (MIT Press).
- Toth, G., Lent, C. S., Tougaw, P. D., Brazhnik, Y., Weng, W., Porod, W., Liu, R.-W. & Huang, Y.-F. [1996] "Quantum cellular neural networks," *Superlatt. Microstruct.* **20**, 473–477.

- Tougaw, P. D., Lent, C. S. & Porod, W. [1993] "Bistable saturation in coupled quantum-dot cells," *J. Appl. Phys.* **74**, 3558–3566.
- Tougaw, P. D. & Lent, C. S. [1994] "Logical devices implemented using quantum cellular automata," *J. Appl. Phys.* **75**, 1818–1825.
- Turton, R. [1995] *The Quantum Dot: A Journey into the Future of Microelectronics* (Oxford University Press).
- Waugh, F. R., Berry, M. J., Mar, D. J., Westervelt, R. M., Campman, K. L. & Goddard, A. C. [1995] "Single-electron charging in double and triple quantum dots with tunable coupling," *Phys. Rev. Lett.* **75**, 705–708.
- Weisbuch, C. & Vinter, B. [1991] *Quantum Semiconductor Structures: Fundamentals and Applications* (Academic Press).
- Wendel, M., Kühn, S., Lorenz, H., Kotthaus, J. P. & Holland, M. [1996] "Nanolithography with an atomic force microscope for integrated fabrication of quantum electronic devices," *Appl. Phys. Lett.* **65**, 1775–1777.
- Zuse, K. [1969] *Rechnender Raum* (Vieweg, Braunschweig); translated as: *Calculating Space* (MIT Technical Translations AZT-70-164-GEMIT, 1970).